Nuclear effects in Drell-Yan pair production in high-energy *pA* collisions

Eduardo Basso,[1,*] Victor P. Goncalves,[2,3,†] Michal Krelina,[4,‡] Jan Nemchik,[4,5,§] and Roman Pasechnik[2,‖]

[1]*Instituto de Física, Universidade Federal do Rio de Janeiro, Caixa Postal 68528, Rio de Janeiro, Rio de Janeiro 21941-972, Brazil*

[2]*Department of Astronomy and Theoretical Physics, Lund University, SE-223 62 Lund, Sweden*

[3]*High and Medium Energy Group, Instituto de Física e Matemática, Universidade Federal de Pelotas, Pelotas, Rio Grande do Sol 96010-900, Brazil*

[4]*Czech Technical University in Prague, FNSPE, Břehová 7, 11519 Prague, Czech Republic*

[5]*Institute of Experimental Physics SAS, Watsonova 47, 04001 Košice, Slovakia*

(Received 10 March 2016; published 24 May 2016)

The Drell-Yan (DY) process of dilepton pair production off nuclei is not affected by final state interactions, energy loss, or absorption. A detailed phenomenological study of this process is thus convenient for investigation of the onset of initial-state effects in proton-nucleus (pA) collisions. In this paper, we present a comprehensive analysis of the DY process in pA interactions at RHIC and LHC energies in the color dipole framework. We analyze several effects affecting the nuclear suppression, $R_{pA} < 1$, of dilepton pairs, such as the saturation effects, restrictions imposed by energy conservation (the initial-state effective energy loss), and the gluon shadowing, as a function of the rapidity, the invariant mass of the dileptons, and their transverse momenta p_T. In this analysis, we take into account not only the γ^* but also the Z^0 contribution to the production cross section, thus extending the predictions to large dilepton invariant masses. Besides the nuclear attenuation of produced dileptons at large energies and forward rapidities emerging due to the onset of shadowing effects, we predict a strong suppression at large p_T, dilepton invariant masses, and Feynman variable x_F caused by the initial-state interaction effects in kinematic regions where no shadowing is expected. The manifestations of nuclear effects are also investigated in terms of the correlation function in the azimuthal angle between the dilepton pair and a forward pion $\Delta\phi$ for different energies, dilepton rapidities, and invariant dilepton masses. We predict that the characteristic double-peak structure of the correlation function around $\Delta\phi \simeq \pi$ arises for very forward pions and large-mass dilepton pairs.

DOI: 10.1103/PhysRevD.93.094027

I. INTRODUCTION

During the last two decades, a series of theoretical and experimental studies of particle production in heavy ion collisions (HICs) at Relativistic Heavy Ion Collider (RHIC) and Large Hadrons Collider (LHC) energies has been performed. These results provided us with various sources of information on properties of the hot and dense matter (quark gluon plasma) formed in these collisions. Although several issues still remain open, those are mainly related to a description of nuclear effects related to the initial-state formation before it interacts with a nuclear target, as well as to the parton propagation in a nuclear medium. In this context, the phenomenological studies of hard processes in proton-nucleus (pA) collisions can provide us with additional quantitative information about various nuclear effects expected also in HICs. This can help us to distinguish between the medium effects of different types and constrain their relative magnitudes and contributions [1].

A key feature of the Drell-Yan (DY) process is the absence of final state interactions and fragmentation associated with an energy loss or absorption phenomena. For this reason, the DY process can be considered a very clean probe for the initial-state interaction (ISI) effects [2]. In practice, this process can be used as a convenient tool in studies of the quantum chromodynamics (QCD) at high energies, particularly the saturation effects expected to determine the initial conditions in hadronic collisions, as well as the initial-state energy loss due to the projectile quark propagation in the nuclear medium before it experiences a hard scattering.

In this paper, we study the DY process on nuclear targets at high energies using the color dipole approach [3–12], which is known to give as precise a prediction for the DY cross section as the next-to-leading-order (NLO) collinear factorization framework and allows us to include naturally the coherence effects in nuclear collisions. Moreover, the color dipole formalism provides a straightforward generalization of the DY process description from the proton-proton to proton-nucleus collisions and is thus suitable for

*eduardo.basso@thep.lu.se
†victor.goncalves@thep.lu.se
‡michal.krelina@fjfi.cvut.cz
§nemcik@saske.sk
‖roman.pasechnik@thep.lu.se

studies of nuclear effects directly accessing the impact-parameter dependence of nuclear shadowing and nuclear broadening—the critical information which is not available in the parton model.

In contrast to the conventional parton model, where the dilepton production process is typically viewed as the parton annihilation in the center of mass (c.m.) frame, in the color dipole approach operating in the target rest frame the same process looks as a bremsstrahlung of a γ^*/Z^0 boson off a projectile quark. In pA collisions assuming the high-energy limit, the projectile quark probes a dense gluonic field in the target and the nuclear shadowing leads to a nuclear modification of the transverse momentum distribution of the DY production cross section. The onset of shadowing effects is controlled by the coherence length, which can be interpreted as the mean lifetime of γ^*/Z^0-quark fluctuations, and is given by

$$l_c = \frac{1}{x_2 m_N} \frac{(M_{l\bar{l}}^2 + p_T^2)(1-\alpha)}{\alpha(1-\alpha)M_{l\bar{l}}^2 + \alpha^2 m_f^2 + p_T^2}, \tag{1}$$

where $M_{l\bar{l}}$ is the dilepton invariant mass and p_T its transverse momentum. Moreover, α is the fraction of the light-cone momentum of the projectile quark carried out by the gauge boson. As demonstrated in Fig. 1, in the RHIC and LHC kinematic regions, the coherence length exceeds the nuclear radius R_A, $l_c \gtrsim R_A$, which implies that the long coherence length (LCL) limit can be safely used in practical calculations of the DY cross section in pA collisions.

Besides the quark shadowing effects naturally accounted for in the dipole picture, one should also take into account the nuclear effects due to multiple rescattering of initial-state projectile partons (ISI effects) in a medium before a hard scattering. The latter are important close to the kinematic limits, e.g., at a large Feynman variable $x_F \to 1$ and $x_T = 2p_T/\sqrt{s} \to 1$ ($\sqrt{s}$ is the collision energy in the c.m. frame), due to restrictions imposed by energy conservation. In this paper, we take into account also nonlinear QCD effects, which are amplified in nuclear collisions and related to multiple scatterings of the higher Fock states containing gluons in the dipole-target interactions. They generate the gluon shadowing effects effective at small Bjorken x in the target and large rapidity values.

In our study, all of the basic ingredients for the DY nuclear production cross section [such as the dipole cross section parametrizations and parton distribution functions (PDFs)] have been determined from other processes. Consequently, our predictions are parameter free and should be considered an important test for the onset of distinct nuclear effects. Note that the nuclear DY process mediated by a virtual photon has already been studied within the color dipole framework by several authors (see, e.g., Refs. [7–9]). However, the results of this paper represent a further step by updating and improving the previous analyses in the literature and providing new predictions for the transverse momentum, dilepton invariant mass, and rapidity distributions of the nuclear DY production cross section at RHIC and LHC energies, as well as in comparison to the most recent data. In addition, the effects of quantum coherence at large energies—including the gluon shadowing as a leading-twist shadowing correction as well as an additional contribution of the Z^0 boson and γ^*/Z^0 interference—are incorporated. Moreover, the impact of the effective initial-state energy loss effects on the DY nuclear production cross section is studied for the first time. We also investigate nuclear effects providing a detailed analysis of the azimuthal correlation between the produced DY pair and a forward pion, taking into account the Z^0 boson contribution in addition to the virtual photon, thus generalizing the results presented in Ref. [13].

This paper is organized as follows. In Sec. II, we present a brief overview of gauge boson production in the color dipole framework. Moreover, we discuss in detail the saturation effects, gluon shadowing, and initial-state energy loss effects included in the analysis. Section III is devoted to predictions for the dilepton invariant mass,

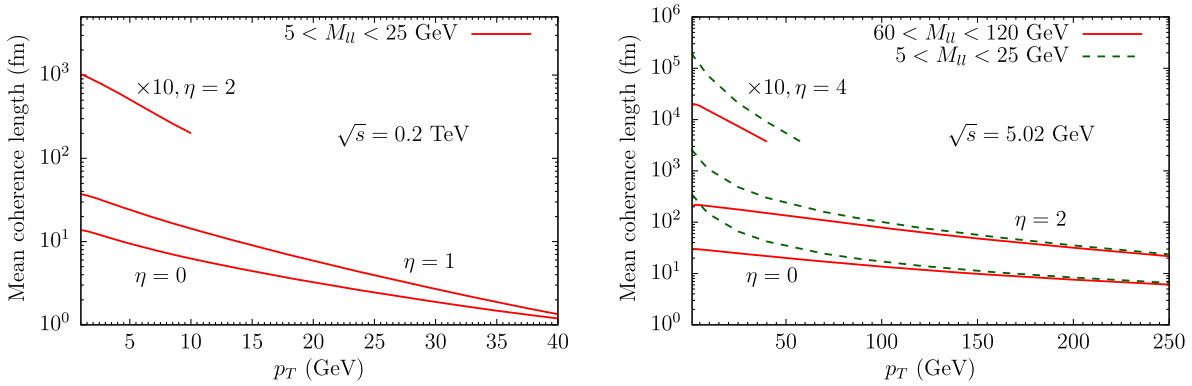

FIG. 1. The mean coherence length l_c of the DY reaction in pA collisions at RHIC and LHC energies for different dilepton rapidities and invariant mass ranges.

rapidity, and transverse momentum distributions of the DY nuclear production cross sections in comparison with the available data. The onset of various nuclear effects is estimated in the LCL limit and the predictions for the nucleus-to-nucleon ratio, $R_{pA} = \sigma_{pA}/A\sigma_{pp}$,[1] of the DY production cross sections are presented. The latter can be verified in the future by experiments at the RHIC and the LHC. Furthermore, the azimuthal correlation function between the produced dilepton and a pion is evaluated for pA collisions at the RHIC and the LHC for different dilepton invariant masses, including the high-mass region. Finally, in Sec. IV we summarize our main conclusions.

II. DRELL-YAN PROCESS IN HADRON-NUCLEUS COLLISIONS

A. DY nuclear cross section

The color dipole formalism is treated in the target rest frame where the process of DY pair production can be viewed as a radiation of gauge bosons $G^* = \gamma^*/Z^0$ by a projectile quark (see, e.g., Refs. [10,12]). Assuming only the lowest $|qG^*\rangle$ Fock component, the cross section for the inclusive gauge boson production with invariant mass $M_{l\bar{l}}$ and transverse momentum p_T can be expressed in terms of the projectile quark (antiquark) densities q_f ($\bar{q}_f$) at momentum fraction x_q and the quark-nucleus cross section as follows (see, e.g., Refs. [7,12]):

$$\frac{d\sigma(pA \to G^*X)}{\mathrm{d}^2 p_T d\eta} = J(\eta, p_T)\frac{x_1}{x_1+x_2}\sum_f \sum_{\lambda_G = L,T}\int_{x_1}^1 \frac{d\alpha}{\alpha^2}[q_f(x_q,\mu_F^2) + \bar{q}_f(x_q,\mu_F^2)]\frac{d\sigma^f_{\lambda_G}(qA \to qG^*X)}{d(\ln\alpha)d^2p_T}, \tag{2}$$

where

$$J(\eta, p_T) \equiv \frac{dx_F}{d\eta} = \frac{2}{\sqrt{s}}\sqrt{M_{l\bar{l}}^2 + p_T^2}\cosh(\eta) \tag{3}$$

is the Jacobian of the transformation between the Feynman variable $x_F = x_1 - x_2$ and the pseudorapidity η of the virtual gauge boson G^*, $x_q = x_1/\alpha$, where α is the fraction of the light-cone momentum of the projectile quark carried out by the gauge boson, and $\mu_F^2 = p_T^2 + (1-x_1)M_{l\bar{l}}^2$ is the factorization scale in quark PDFs. As in Ref. [12], we take $\mu_F \simeq M_{l\bar{l}}$, for simplicity.

The transverse momentum distribution in Eq. (2) of the gauge boson G^* bremsstrahlung in quark-nucleus interactions can be obtained by a generalization of the well-known formulas for the photon bremsstrahlung from Refs. [5,7,8]. Then the corresponding differential cross section for a given incoming quark of flavor f reads

$$\frac{d\sigma^f_{T,L}(qA \to qG^*X)}{d(\ln\alpha)d^2p_T} = \frac{1}{(2\pi)^2}\sum_{\text{quark pol}}\int d^2\rho_1 d^2\rho_2 \exp[i\mathbf{p}_T\cdot(\boldsymbol{\rho}_1 - \boldsymbol{\rho}_2)]\Psi^{\mathcal{V}-\mathcal{A}}_{T,L}(\alpha,\boldsymbol{\rho}_1,m_f)\Psi^{\mathcal{V}-\mathcal{A},*}_{T,L}(\alpha,\boldsymbol{\rho}_2,m_f)$$
$$\times\frac{1}{2}[\sigma^A_{q\bar{q}}(\alpha\boldsymbol{\rho}_1,x_2) + \sigma^A_{q\bar{q}}(\alpha\boldsymbol{\rho}_2,x_2) - \sigma^A_{q\bar{q}}(\alpha|\boldsymbol{\rho}_1 - \boldsymbol{\rho}_2|,x_2)], \tag{4}$$

where $x_2 = x_1 - x_F$ and $\boldsymbol{\rho}_{1,2}$ are the quark-G^* transverse separations in the total radiation amplitude and its conjugated counterpart, respectively. Assuming that the projectile quark is unpolarized, the vector $\Psi^{\mathcal{V}}$ and axial-vector $\Psi^{\mathcal{A}}$ wave functions in Eq. (4) are not correlated, such that

$$\sum_{\text{quark pol}}\Psi^{\mathcal{V}-\mathcal{A}}_{T,L}(\alpha,\boldsymbol{\rho}_1,m_f)\Psi^{\mathcal{V}-\mathcal{A},*}_{T,L}(\alpha,\boldsymbol{\rho}_2,m_f)$$
$$= \Psi^{\mathcal{V}}_{T,L}(\alpha,\boldsymbol{\rho}_1,m_f)\Psi^{\mathcal{V},*}_{T,L}(\alpha,\boldsymbol{\rho}_2,m_f)$$
$$+ \Psi^{\mathcal{A}}_{T,L}(\alpha,\boldsymbol{\rho}_1,m_f)\Psi^{\mathcal{A},*}_{T,L}(\alpha,\boldsymbol{\rho}_2,m_f), \tag{5}$$

where the averaging over the initial and summation over final quark helicities is performed and the quark flavor dependence comes only via the projectile quark mass m_f. The corresponding wave functions $\Psi^{\mathcal{V}-\mathcal{A}}_{T,L}(\alpha,\boldsymbol{\rho})$ can be found in Ref. [10].

Our goal is to evaluate the DY production cross section in pA collisions at high energies and a large-mass number A of the nuclear target. This regime is characterized by a limitation on the maximum phase-space parton density that can be reached in the hadron wave function (parton saturation) [14]. The transition between the linear and nonlinear regimes of QCD dynamics is typically specified by a characteristic energy-dependent scale called the saturation scale Q_s^2, where the variable s denotes the c.m. energy of the collision squared. We expect such

[1]Here, A represents the atomic mass number of the nuclear target.

saturation effects to be amplified in nuclear collisions since the nuclear saturation scale $Q^2_{s,A}$ is expected to be enlarged with respect to the nucleon one $Q^2_{s,p}$ by approximately a factor of $A^{1/3}$.

In general, the dipole-nucleus cross section $\sigma^A_{q\bar{q}}(\rho, x)$ can be written in terms of the forward dipole-nucleus scattering amplitude $\mathcal{N}^A(\rho, x, \boldsymbol{b})$ as follows:

$$\sigma^A_{q\bar{q}}(\boldsymbol{\rho}, x) = 2\int d^2\boldsymbol{b}\mathcal{N}^A(\boldsymbol{\rho}, x, \boldsymbol{b}). \tag{6}$$

At high energies, the evolution of $\mathcal{N}^A(x, \boldsymbol{r}, \boldsymbol{b})$ in the rapidity $Y = \ln(1/x)$ is given, for example, within the color glass condensate (CGC) formalism [15], in terms of an infinite hierarchy of equations known as the so-called Balitsky-JIMWLK equations [15,16], which reduces in the mean field approximation to the Balitsky-Kovchegov (BK) equation [16,17]. In recent years, several groups have studied the solution of the BK equation, taking into account the running coupling corrections to the evolution kernel. However, these analyses have assumed the translational invariance approximation, which implies that $\mathcal{N}^A(\rho,x,\boldsymbol{b}) = \mathcal{N}^A(\rho,x)S(\boldsymbol{b})$ and $\sigma^A_{q\bar{q}}(\boldsymbol{\rho}, x, \boldsymbol{b}) = \sigma_0\mathcal{N}(\rho, x)$, where $\mathcal{N}(\rho, x)$ is a partial dipole amplitude on a nucleon, and σ_0 is the normalization of the dipole cross section fitted to the data. Basically, they disregard the impact-parameter dependence. Unfortunately, the impact-parameter dependent numerical solutions of the BK equation are very difficult to obtain [18]. Moreover, the choice of the impact-parameter profile of the dipole amplitude entails an intrinsically nonperturbative physics, which is beyond the QCD weak coupling approach of the BK equation. In what follows, we explore an alternative path and employ the available phenomenological models, which explicitly incorporate an expected b dependence of the scattering amplitude.

B. Models for the dipole cross section

As in our previous studies [19–24], we work in the LCL limit and employ the model initially proposed in Ref. [25] which includes the impact-parameter dependence in the dipole-nucleus amplitude and describes the experimental data on the nuclear structure function (for more details, see Refs. [19,26]). In particular, this model enables us to incorporate the shadowing effects via a simple eikonalization of the standard dipole-nucleon cross section $\sigma_{q\bar{q}}(\boldsymbol{\rho}, x)$, such that the forward dipole-nucleus amplitude in Eq. (6) is given by

$$\mathcal{N}^A(\boldsymbol{\rho}, x, \boldsymbol{b}) = 1 - \exp\left(-\frac{1}{2}T_A(\boldsymbol{b})\sigma_{q\bar{q}}(\boldsymbol{\rho}, x)\right), \tag{7}$$

where $T_A(\boldsymbol{b})$ is the nuclear profile (thickness) function, which is normalized to the mass number A and reads

$$T_A(\boldsymbol{b}) = \int_{-\infty}^{\infty}\rho_A(\boldsymbol{b}, z)dz. \tag{8}$$

Here, $\rho_A(\boldsymbol{b}, z)$ represents the nuclear density function defined at the impact parameter $\boldsymbol{b}$ and the longitudinal coordinate z. In our calculations we used realistic parametrizations of $\rho_A(\boldsymbol{b}, z)$ from Ref. [27]. The eikonal formula (7) based upon the Glauber-Gribov formalism [28] resums the multiple elastic rescattering diagrams of the $q\bar{q}$ dipole in a nucleus in the high-energy limit. The eikonalization procedure is justified in the LCL regime where the transverse separation ρ of partons in the multiparton Fock state of the photon is frozen during propagation through the nuclear matter and becomes an eigenvalue of the scattering matrix.

For the numerical analysis of the nuclear DY observables, we need to specify a reliable parametrization for the dipole-proton cross section. In recent years, several groups have constructed a number of viable phenomenological models based on saturation physics and fits to the HERA and RHIC data (see, e.g., Refs. [29–41]).

As in our previous study of the DY process in pp collisions [12], in order to estimate theoretical uncertainty in our analysis, in what follows, we consider several phenomenological models for the dipole cross section $\sigma_{q\bar{q}}$ which take into account the DGLAP evolution, as well as the saturation effects.

The first one is the model proposed in Ref. [38], where the dipole cross section is given by

$$\sigma_{q\bar{q}}(\boldsymbol{\rho}, x) = \sigma_0\left[1 - \exp\left(-\frac{\pi^2}{\sigma_0 N_c}\rho^2\alpha_s(\mu^2)xg(x, \mu^2)\right)\right], \tag{9}$$

where $N_c = 3$ is the number of colors, $\alpha_s(\mu^2)$ is the strong coupling constant at the μ scale, which is related to the dipole size ρ as $\mu^2 = C/\rho^2 + \mu_0^2$, with the C, μ_0, and σ_0 parameters fitted to the HERA data. Moreover, in this model the gluon density evolves according to the Dokshitzer-Gribov-Lipatov-Altarelli-Parisi (DGLAP) equation [42], accounting for gluon splittings only,

$$\frac{\partial xg(x, \mu^2)}{\partial \ln \mu^2} = \frac{\alpha_s(\mu^2)}{2\pi}\int_x^1 dz P_{gg}(z)\frac{x}{z}g\left(\frac{x}{z}, \mu^2\right), \tag{10}$$

where the gluon density at the initial scale μ_0^2 is parametrized as [38]

$$xg(x, \mu_0^2) = A_g x^{-\lambda_g}(1 - x)^{5.6}. \tag{11}$$

The set of best fit values of the model parameters reads $A_g = 1.2$, $\lambda_g = 0.28$, $\mu_0^2 = 0.52$ GeV^2, $C = 0.26$, and $\sigma_0 = 23$ mb. In what follows, we denote by BGBK the predictions for the DY observables obtained using Eq. (9)

as an input in calculations of the dipole-nucleus scattering amplitude.

The model proposed in Ref. [38] was generalized in Ref. [35] in order to take into account the impact-parameter dependence of the dipole-proton cross section and to describe the exclusive observables at HERA. In this model, the corresponding dipole-proton cross section is given by

$$\sigma_{q\bar{q}}(\boldsymbol{\rho},x) = 2\int d^2b_p \left[1-\exp\left(-\frac{\pi^2}{2N_c}\rho^2\alpha_s(\mu^2)xg(x,\mu^2)T_G(\mathbf{b}_p)\right)\right], \tag{12}$$

with the DGLAP evolution of the gluon distribution given by Eq. (10). The Gaussian impact-parameter dependence is given by $T_G(\mathbf{b_p}) = (1/2\pi B_G)\exp(-b_p^2/2B_G)$, where B_G is a free parameter extracted from the t dependence of the exclusive electron-proton (ep) data. The parameters of this model were updated in Ref. [40] by fitting to the recent high precision HERA data [43], providing the following values: $A_g = 2.373$, $\lambda_g = 0.052$, $\mu_0^2 = 1.428$ GeV^2, $B_G = 4.0$ GeV^2, and $C = 4.0$. Hereafter, we will denote as IP-SAT the resulting predictions obtained using Eq. (12) as an input in calculations of $\mathcal{N}^A$, Eq. (7).

For comparison with the previous results existing in the literature, we also consider the Golec-Biernat-Wusthoff (GBW) model [29] based upon a simplified saturated form,

$$\sigma_{q\bar{q}}(\boldsymbol{\rho},x) = \sigma_0\left(1-e^{-\frac{\rho^2Q_s^2(x)}{4}}\right), \tag{13}$$

with the saturation scale

$$Q_s^2(x) = Q_0^2\left(\frac{x_0}{x}\right)^{\lambda}, \tag{14}$$

where the model parameters $Q_0^2 = 1$ GeV^2, $x_0 = 4.01\times10^{-5}$, $\lambda = 0.277$, and $\sigma_0 = 29$ mb were obtained from the fit to the deep inelastic scattering (DIS) data accounting for a contribution of the charm quark.

Finally, we also consider the running coupling solution of the BK equation for the partial dipole amplitude obtained in Ref. [44] using the GBW model as an initial condition, such that $\sigma^p_{q\bar{q}}(\boldsymbol{\rho},x) = \sigma_0\mathcal{N}^p(\boldsymbol{\rho},x)$, where the normalization σ_0 is fitted to the HERA data.

C. Gluon shadowing corrections

In the LHC energy range, the eikonal formula for the LCL regime, Eq. (7), is not exact. Besides the lowest $|qG^*\rangle$ Fock state, where $G^* = \gamma^*/Z^0$, one should include also the higher Fock components containing gluons, e.g., $|qG^*g\rangle$, $|qG^*gg\rangle$, etc. They cause an additional suppression known as gluon shadowing (GS). Such high LHC energies allow us to activate the coherence effects also for these gluon fluctuations, which are heavier and consequently have a shorter coherence length than the lowest Fock component, $|qG^*\rangle$. The corresponding suppression factor R_G, as the ratio of the gluon densities in nuclei and nucleon, was derived in Ref. [45] using the Green function technique through the calculation of the inelastic correction $\Delta\sigma_{\rm tot}(q\bar{q}g)$ to the total cross section $\sigma_{\rm tot}^{\gamma^*A}$, related to the creation of a $|q\bar{q}g\rangle$ intermediate Fock state

$$R_G(x,Q^2,\boldsymbol{b}) \equiv \frac{xg_A(x,Q^2,\boldsymbol{b})}{A\cdot xg_p(x,Q^2)} \approx 1-\frac{\Delta\sigma_{\rm tot}(q\bar{q}g)}{\sigma_{\rm tot}^{\gamma^*A}}. \tag{15}$$

GS corrections are included in calculations replacing $\sigma^N_{q\bar{q}}(\boldsymbol{\rho},x) \to \sigma^N_{q\bar{q}}(\boldsymbol{\rho},x)R_G(x,Q^2,\boldsymbol{b})$. They lead to additional nuclear suppression in the production of DY pairs at the small Bjorken $x = x_2$ in the target. In Fig. 2 (left panel) we present our results for the x dependence of the ratio $R_G(x,Q^2,\boldsymbol{b})$ for different vales of the impact parameter b. As expected, the magnitude of the shadowing corrections decreases at large values of b. In the right panel we present our predictions for the b-integrated nuclear ratio $R_G(x,Q^2)$ for different values of the hard scale Q^2. This figure shows

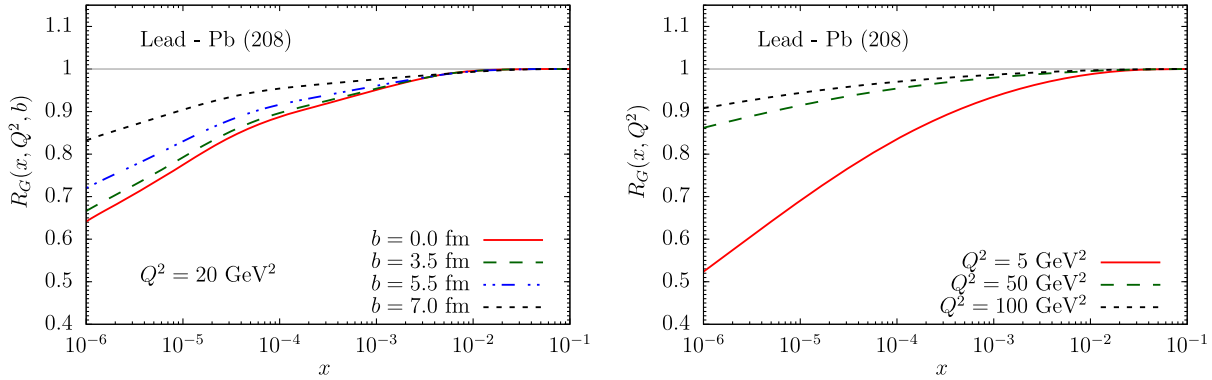

FIG. 2. (Left panel) The x dependence of the ratio $R_G(x,Q^2,\boldsymbol{b})$ for different values of the impact parameter. (Right panel) The x dependence of the b-integrated ratio $R_G(x,Q^2)$ for distinct values of the hard scale Q^2.

a not very strong onset of GS, which was confirmed by the NLO global analyses of DIS data [46]. A weak Q^2 dependence of GS demonstrates that GS is a leading-twist effect, with $R_G(x,Q^2)$ approaching unity only very slowly (logarithmically) as $Q^2 \to \infty$.

D. Effective energy loss

The effective initial-state energy loss (ISI effects) is expected to suppress noticeably the nuclear cross section when reaching the kinematical limits,

$$x_L = \frac{2p_L}{\sqrt{s}} \to 1, \qquad x_T = \frac{2p_T}{\sqrt{s}} \to 1.$$

Correspondingly, a proper variable which controls this effect is $\xi = \sqrt{x_L^2 + x_T^2}$. The magnitude of suppression was evaluated in Ref. [47]. It was found within the Glauber approximation that each interaction in the nucleus leads to a suppression factor $S(\xi) \approx 1 - \xi$. Summing up over the multiple initial-state interactions in a pA collision at impact parameter b, one arrives at a nuclear ISI-modified PDF,

$$q_f(x,Q^2) \Rightarrow q_f^A(x,Q^2,b) = C_v q_f(x,Q^2) \frac{e^{-\xi\sigma_{\rm eff}T_A(b)} - e^{-\sigma_{\rm eff}T_A(b)}}{(1-\xi)(1-e^{-\sigma_{\rm eff}T_A(b)})}. \quad (16)$$

Here, $\sigma_{\rm eff} = 20$ mb is the effective hadronic cross section controlling the multiple interactions. The normalization factor C_v is fixed by the Gottfried sum rule (for more details, see Ref. [47]). It was found that such an additional nuclear suppression emerging due to the ISI effects represents an energy independent feature common for all known reactions experimentally studied so far, with any leading particle (hadrons, Drell-Yan dileptons, charmonium, etc). Specifically, such a suppression was indicated at midrapidity, $y = 0$, and at large p_T by the PHENIX data [48] on π^0 production in central dAu collisions and on direct photon production in central $AuAu$ collisions [49], where no shadowing is expected since the corresponding Bjorken $x = x_2$ in the target is large. Besides large p_T values, the same mechanism of nuclear attenuation is effective also at forward rapidities (large Feynman variable x_F), where we expect a much stronger onset of nuclear suppression, as was demonstrated by the BRAHMS and STAR data [50]. In our case, we predict that the ISI effects induce a significant suppression of the DY nuclear cross section at large dilepton p_T and dilepton invariant mass, and at forward rapidities, as one can see in the next section.

III. RESULTS

In what follows, we present our predictions for the DY pair production cross section in the process $pA \to \gamma^*/Z^0 \to l\bar{l}$ obtained within the color dipole formalism and taking into account the medium effects discussed in the previous section. Following Ref. [29], we use the quark mass values to be $m_u = m_d = m_s = 0.14$ GeV, $m_c = 1.4$ GeV, and $m_b = 4.5$ GeV. Moreover, we take the factorization scale μ_F defined above to be equal to the dilepton invariant mass, $M_{l\bar{l}}$, and employ the CT10 NLO parametrization for the projectile quark PDFs [51] (both sea and valence quarks are included). As was demonstrated in Refs. [12,52], there is little sensitivity of DY predictions on PDF parametrization in pp collisions at high energies, so we do not vary the projectile quark PDFs.

In Fig. 3 we compare our predictions for the DY nuclear cross section with available LHC data [53,54] for large invariant dilepton masses, $60 < M_{l\bar{l}} < 120$ GeV, taking into account the saturation effects. In the top panels, we test the predictions of various models for the dipole cross section, comparing them with the experimental data for the rapidity and transverse momentum distributions of the DY production cross sections in pA collisions. As was already verified in Ref. [12] for DY production in pp collisions, the dipole approach works fairly well in description of the current experimental data at high energies. In particular, the BGBK model provides a consistent prediction describing the data on the rapidity distribution quite well in the full kinematical range. In the bottom panels of Fig. 3, we took the BGBK model and considered the impact of gluon shadowing corrections as well as the initial-state effective energy loss (ISI effects), Eq. (16). In the range of large dilepton invariant masses considered, the gluon shadowing corrections are rather small since the corresponding Bjorken $x = x_2$ in the target becomes large. On the other hand, the ISI effects significantly modify the behavior of the rapidity distribution at a large $\eta > 2$. Unfortunately, the current data are not able at this moment to verify the predicted strong onset of ISI effects due to large error bars. In the case of the transverse momentum distribution for large invariant masses and $0 \le \eta \le 2$, the impact of both the gluon shadowing and the ISI effects is negligible.

In order to quantify the impact of the nuclear effects, in what follows, we estimate the invariant mass, rapidity, and transverse momentum dependence of the nucleus-to-nucleon ratio of the DY production cross sections (nuclear modification factor), $R_{pA} = \sigma_{pA}^{\rm DY}/(A \cdot \sigma_{pp}^{\rm DY})$, considering the DY process at the RHIC ($\sqrt{s} = 0.2$ TeV) and LHC ($\sqrt{s} = 5.02$ TeV) energies. The color dipole predictions for the DY production cross section in pp collisions were discussed in detail in Ref. [12]. For consistency, the numerator and the denominator of the nuclear modification factor are evaluated within the same model for the dipole cross section as an input.

In Fig. 4 we present our predictions for the dilepton invariant mass dependence of the ratio $R_{pA}(M_{l\bar{l}})$ at RHIC considering both central and forward rapidities. In the top panels, we show that the dipole model predictions are almost insensitive to the parametrizations used to treat the dipole-proton interactions. The magnitude of the saturation

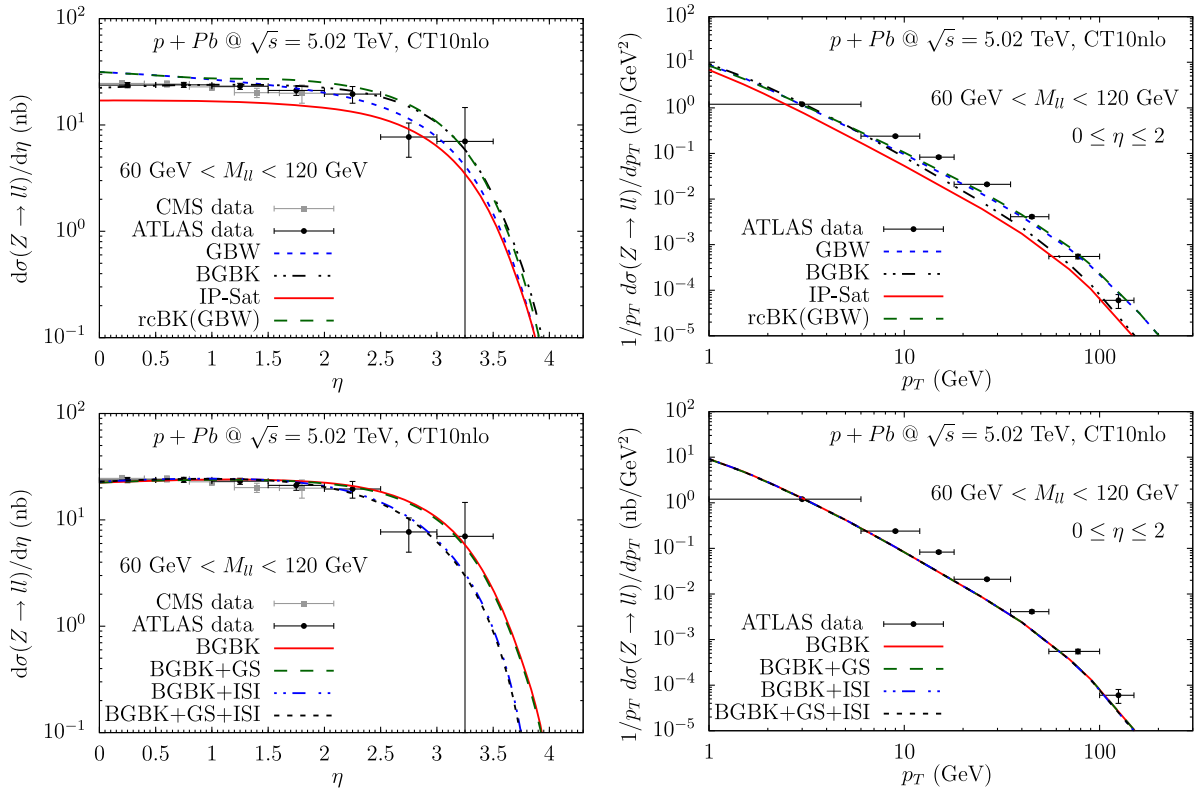

FIG. 3. The dipole model predictions for the DY nuclear cross sections at large dilepton invariant masses compared to the recent experimental data from ATLAS and CMS experiments [53,54] at c.m. collision energy $\sqrt{s} = 5.02$ TeV. The predictions obtained for several parametrizations of the dipole cross section described in the text are shown in the top panels, while the effects of the gluon shadowing and the initial-state energy loss are demonstrated in the bottom panels.

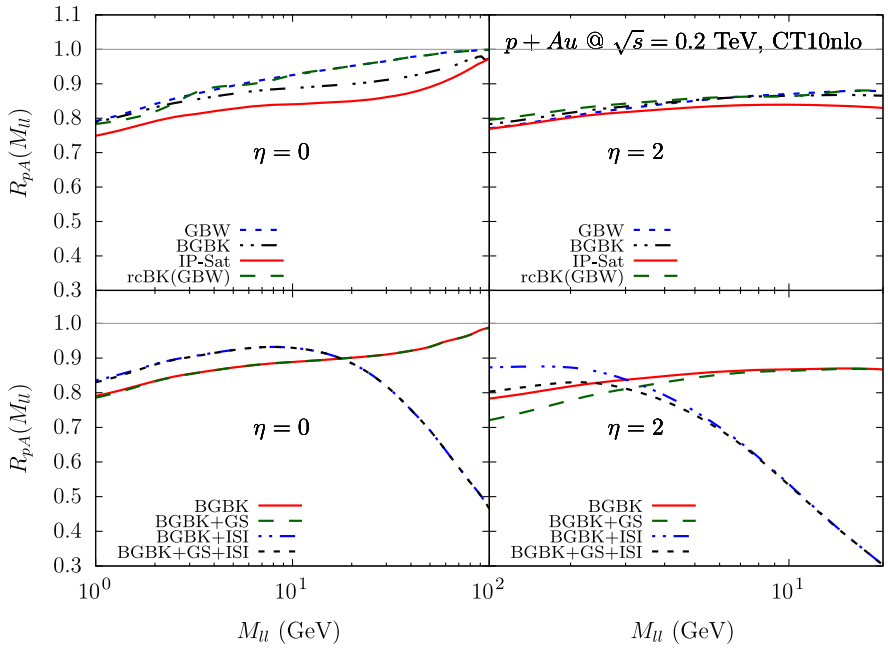

FIG. 4. The dilepton invariant mass dependence of the nucleus-to-nucleon ratio, $R_{pA} = \sigma_{pA}^{\mathrm{DY}}/(A \cdot \sigma_{pp}^{\mathrm{DY}})$, of the DY production cross sections for c.m. energy $\sqrt{s} = 0.2$ TeV corresponding to RHIC experiments.

effects decreases at large dilepton invariant masses and increases at forward rapidities. Such a behavior is expected since at a smaller $M_{l\bar{l}}$ and at a larger η one probes smaller values of the Bjorken-x_2 variable in the target. In the bottom panels of Fig. 4, we present the predictions, taking into account also the GS corrections and the ISI effects. As was mentioned above, we predict a weak onset of GS corrections at central rapidities, whereas GS leads to a significant suppression in the forward region. Besides, as expected, the impact of GS effects decreases with $M_{l\bar{l}}$ due to a rise of the Bjorken-x_2 values. Contrastingly, the ISI effects become effective, causing a strong nuclear suppression at a large $M_{l\bar{l}}$ and/or η. This behavior is also well understood since large dilepton invariant masses and/or rapidities correspond to a large Feynman variable x_F leading to a stronger onset of ISI effects, as follows from Eq. (16). A similar behavior has been predicted for the LHC energy range, as is shown in Fig. 5, where the impact of saturation and GS effects is even more pronounced.

In Fig. 6 we present our predictions for rapidity dependence of the nucleus-to-nucleon ratio, $R_{pA}(\eta)$, of the DY production cross sections at RHIC and LHC energies considering two ranges, $(5 < M_{l\bar{l}} < 25$ GeV) and $(60 < M_{l\bar{l}} < 120$ GeV), of dilepton invariant mass. We would like to emphasize that the onset of saturation effects reduces $R_{pA}(\eta)$ at large rapidities and has a larger impact in the small invariant mass range. For large invariant masses, we predict a reduction of $\approx 10\%$ in the R_{pPb} ratio at the LHC energy. At the RHIC energy we predict a weak onset of GS effects—even at a large $\eta > 3$. In contrast to the RHIC energy range, at the LHC the GS effects lead to a significant additional suppression, modifying thus the ratio R_{pPb}, especially at small dilepton invariant masses and large rapidity values. On the other hand, the onset of the ISI effects is rather strong for both the RHIC and LHC kinematic regions, and it becomes even stronger at forward rapidities for both invariant mass ranges. This makes the phenomenological studies of the rapidity dependence of R_{pA} ideal for constraining such effects.

Fig. 7 shows our predictions for the transverse momentum dependence of the nuclear modification factor, $R_{pA}(p_T)$, for the invariant mass range $5 < M_{l\bar{l}} < 25$ GeV at the RHIC c.m. energy $\sqrt{s} = 0.2$ TeV and two distinct pseudorapidity values, $\eta = 0$ and $\eta = 1$. At large transverse momenta, the role of the saturation effects is negligibly small and can be important only at a small $p_T \leq 2$ GeV. Similarly, the GS effects are almost irrelevant at RHIC energies. However, Fig. 7 clearly demonstrates a strong onset of ISI effects causing a significant suppression at large p_T, where no coherence effects are expected. In accordance with Eq. (16) and in comparison with $\eta = 0$, we predict stronger ISI effects at forward rapidities, as depicted in Fig. 7 for $\eta = 1$. Because of a significant elimination of coherence effects, the study of the DY process at large p_T in pA collisions at RHIC is a very convenient tool for the investigation of net ISI effects. On the other hand, at LHC energies (see Fig. 8) the manifestation of the saturation and GS effects rises at forward rapidities and becomes noticeable for $p_T \leq 10$ GeV. As was already mentioned for RHIC energies, the ISI effects cause a significant attenuation at large transverse momenta and forward rapidities, although no substantial suppression is expected in the DY

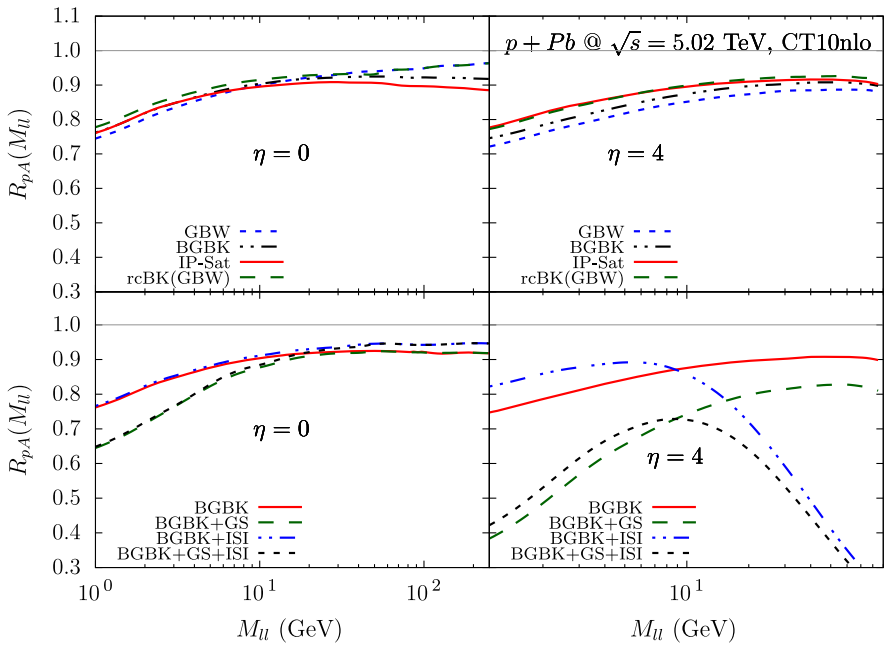

FIG. 5. The dilepton invariant mass dependence of the nucleus-to-nucleon ratio, $R_{pA} = \sigma_{pA}^{\mathrm{DY}}/(A \cdot \sigma_{pp}^{\mathrm{DY}})$, of the DY production cross sections for c.m. energy $\sqrt{s} = 5.02$ TeV corresponding to LHC experiments.

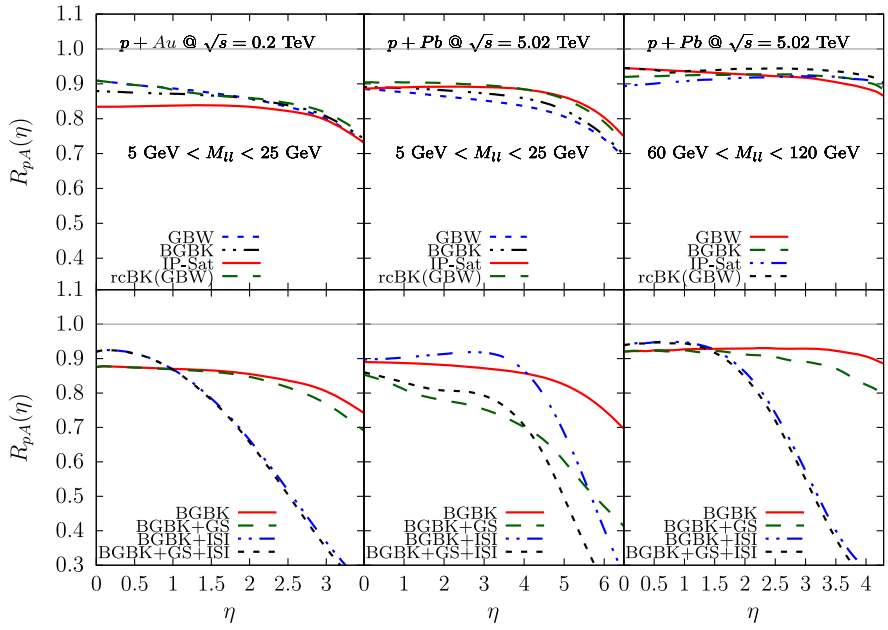

FIG. 6. The pseudorapidity dependence of the nucleus-to-nucleon ratio, $R_{pA}(\eta)$, of the DY production cross sections at the RHIC and LHC energies for two ranges ($5 < M_{l\bar{l}} < 25$ GeV) and ($60 < M_{l\bar{l}} < 120$ GeV) of dilepton invariant mass.

process due to the absence of a final state interaction, energy loss, or absorption. For these reasons, a study of the ratio $R_{pA}(p_T)$, also at the LHC—especially at large p_T and at a small invariant mass range—is very effective for constraining the ISI effects.

In order to reduce the contribution of coherence effects (gluon shadowing, CGC) in the LHC kinematic region, one should go to the range of large dilepton invariant masses, as is shown in Fig. 9. Here, we present our predictions for the ratio $R_{pPb}(p_T)$ at the LHC c.m. collision energy $\sqrt{s}=5.02$ TeV for the range $60 < M_{l\bar{l}} < 120$ GeV and several values of $\eta = 0$, 2, 4. According to expectations, we have found that the saturation and GS effects turn out to be important only at small p_T and a large η. Such an elimination of coherence effects taking into account larger dilepton invariant masses causes simultaneously a stronger

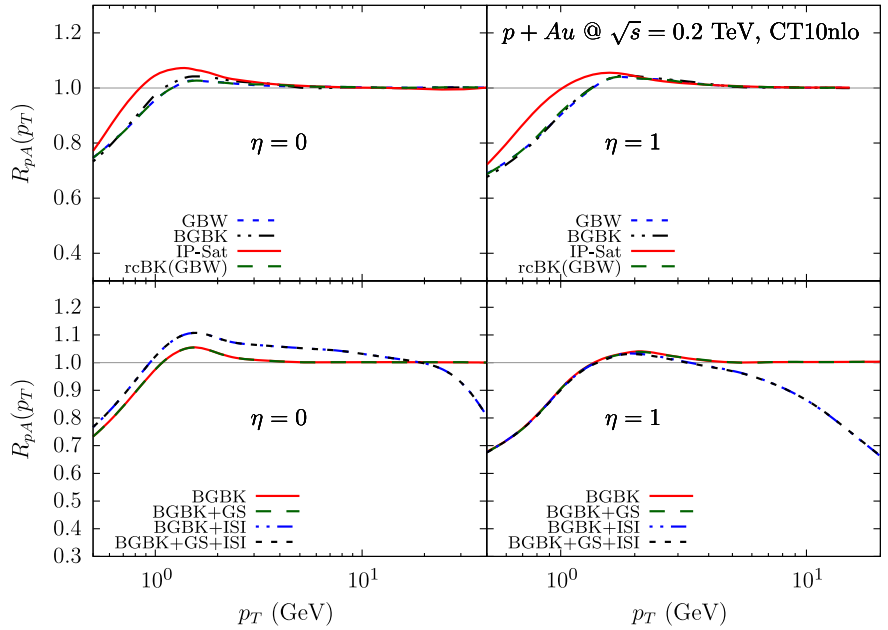

FIG. 7. The transverse momentum dependence of the nucleus-to-nucleon ratio of the DY production cross sections, $R_{pA}(p_T)$, for the dilepton invariant mass range $5 < M_{l\bar{l}} < 25$ GeV at $\sqrt{s}=0.2$ TeV and $\eta = 0$, 1.

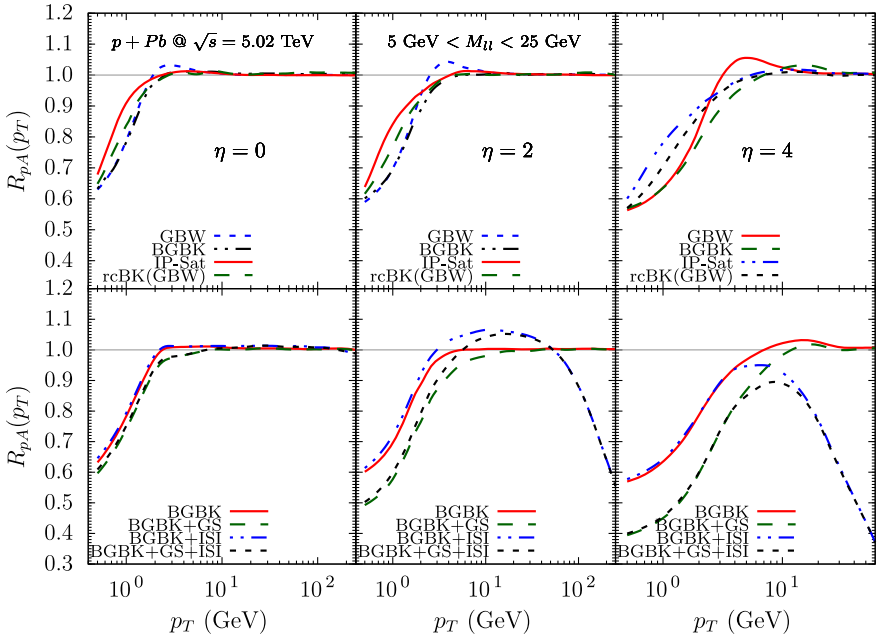

FIG. 8. The transverse momentum dependence of the nucleus-to-nucleon ratio of the DY production cross sections, $R_{pA}(p_T)$, for the dilepton invariant mass range $5 < M_{l\bar{l}} < 25$ GeV at $\sqrt{s} = 5.02$ TeV and $\eta = 0$, 2, 4.

onset of ISI effects, as one can see in Fig. 9 in comparison with Fig. 8. For this reason, an investigation of net ISI effects at a large $M_{l\bar{l}}$ does not require such high p_T and rapidity values, which allows us to obtain the experimental data of higher statistics and, consequently, with smaller error bars. Figure 9 again demonstrates a large nuclear suppression in the forward region ($\eta = 4$) over an extended range of the dilepton transverse momenta. Consequently, such an analysis of the DY nuclear cross section at forward rapidities by, e.g., the LHCb Collaboration can be very useful for probing the ISI effects experimentally.

Finally, let us discuss the azimuthal correlation between the DY pair and a forward pion produced in pA collisions, taking into account the Z^0 boson contribution in addition

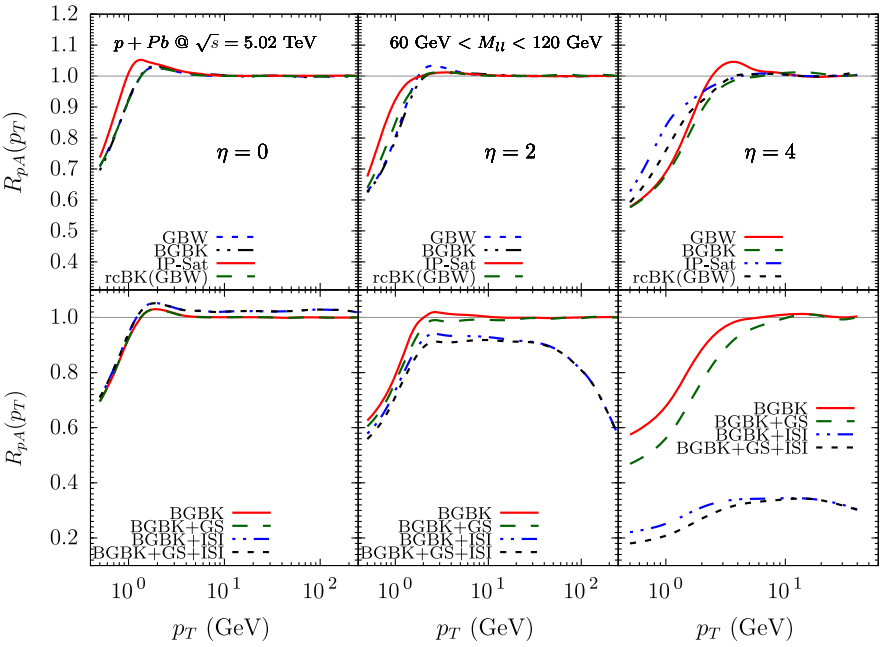

FIG. 9. The transverse momentum dependence of the nucleus-to-nucleon ratio of the DY production cross sections, $R_{pA}(p_T)$, for the dilepton invariant mass range $60 < M_{l\bar{l}} < 120$ GeV at $\sqrt{s} = 5.02$ TeV and $\eta = 0$, 2, 4.

to the virtual photon, as well as the saturation effects. As was discussed earlier in Refs. [12,13,55], the dilepton-hadron correlations can serve as an efficient probe of the initial-state effects. The gauge boson radiation off the projectile quark has a back-to-back correlation in the transverse momentum. However, the multiple scatterings of the quark in a high density gluonic system implies that it acquires a transverse momentum comparable to the saturation scale. As a consequence, we expect the intrinsic angular correlations to be suppressed, with the suppression being directly related to the magnitude of the saturation scale. As the saturation scale is strongly dependent on the nuclear atomic number, we expect that the effects predicted in Ref. [12] for the DY process in pp collisions to be amplified in the pA case. Considering the $G^* = \gamma^*/Z_0$ boson as a trigger particle, the corresponding correlation function can be written

$$C(\Delta\phi) = \frac{2\pi \int_{p_T, p_T^h > p_T^{\rm cut}} dp_T p_T dp_T^h p_T^h \frac{d\sigma(pA\to hG^*X)}{dY dy_h d^2p_T d^2p_T^h}}{\int_{p_T > p_T^{\rm cut}} dp_T p_T \frac{d\sigma(pA\to G^*X)}{dY d^2p_T}}, \quad (17)$$

where $p_T^{\rm cut}$ is the experimental low cutoff on transverse momenta of the resolved G^* (or dilepton) and a hadron h, and $\Delta\phi$ is the angle between them. The differential cross sections entering the numerator and the denominator of $C(\Delta\phi)$ have been derived for pp collisions in Ref. [12], taking into account both the γ^* and Z^0 boson contributions, and they can now be directly generalized for pA collisions by accounting the nuclear dependence of the saturation scale. We refer to Ref. [12] for details of the differential cross sections. The main input in the calculation of the correlation function is the unintegrated gluon distribution $F(x_g, k_T^g)$, where x_g and k_T^g are the momentum fraction and the transverse momentum of the target gluon, which is directly associated with the description of the QCD dynamics in the high-energy limit [14]. As demonstrated in Ref. [13], the correlation function for $\Delta\phi \approx \pi$ is determined by the low-k_T^g behavior of the unintegrated gluon distribution, which is strongly associated with the saturation effects. Since in this regime the current parametrizations for $F(x_g, k_T^g)$ are similar, the resulting predictions for $C(\Delta\phi \approx \pi)$ are almost model independent. In order to compare our predictions with those presented in Refs. [12,13], in what follows we study the correlation function $C(\Delta\phi)$, taking the unintegrated gluon distribution in the following form:

$$F(x_g, k_T^g) = \frac{1}{\pi Q_{s,A}^2(x_g)} e^{-k_T^{g\,2}/Q_{s,A}^2(x_g)}, \quad (18)$$

where $Q_{s,A}^2(x) = A^{1/3} c(b) Q_{s,p}^2(x)$ is the saturation scale and $Q_{s,p}^2(x)$ is given by Eq. (14). In numerical analysis, the CT10 NLO parametrization [51] for the parton distributions and the Kniehl-Kramer-Potter fragmentation function $D_{h/f}(z_h, \mu_F^2)$ of a quark to a neutral pion [56] have been used. Moreover, we assume that the minimal transverse momentum ($p_T^{\rm cut}$) of the gauge boson G^* and the pion $h = \pi$ in Eq. (17) are the same and equal to 1.5 and 3.0 GeV for the RHIC and LHC energies, respectively. As in our previous study [12], we assume that the factorization scale is given by the dilepton invariant mass, i.e., $\mu_F = M_{l\bar{l}}$.

The analysis of the correlation function in the pp collisions performed in Ref. [12] has demonstrated that an increase of the saturation scale at large rapidities implies a larger value for the transverse momentum carried by the low-x gluons in the target which generates the decorrelation between the back-to-back jets. Since the magnitude of the saturation scale is amplified by the factor $A^{1/3}$ in nuclear collisions we should also expect a similar effect in pA collisions. In particular, the double-peak structure of $C(\Delta\phi)$ in the away-side dilepton-pion angular correlation function predicted to be present in pp collisions [12] should also occur in the pA case. As discussed in detail in Refs. [12,13,55], this double peak in the region where $\Delta\phi \approx \pi$ is directly associated with the interplay between the local minimum of the $h + G$ cross section for gluon $k_T^g = |\vec{p}_T + \vec{p}_{Tq}| \to 0$, where $\vec{p}_T$ ($\vec{p}_{Tq}$) is the transverse momentum of the gauge boson (quark), and the two maxima for the cross section when $k_T \to Q_s$. Therefore, the double-peak structure is sensitive to the magnitude of the saturation scale as well. In Fig. 10 we present our predictions for the correlation function $C(\Delta\phi)$ of the associated DY pair and pion in pA collisions at LHC energies, considering different values of the atomic mass number. We notice that the larger values of A imply the stronger smearing of the back-to-back scattering pattern and suppress the away-side peak in the $\Delta\phi$ distribution. This behavior is expected since in high-energy collisions the produced parton has, on average, intrinsic transverse momentum of the order of the saturation scale which increases for larger A. Such an increase in Q_s washes away the intrinsic back-to-back correlations. Moreover, at a

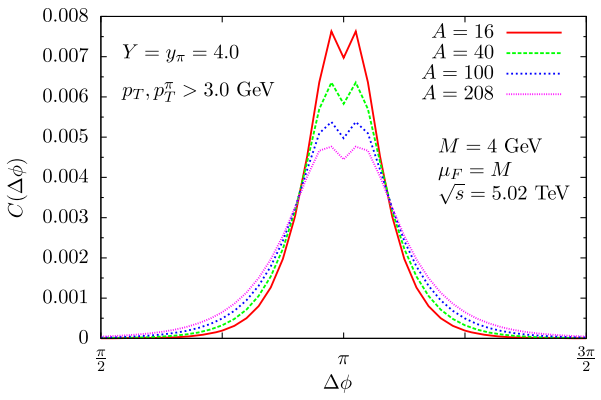

FIG. 10. The correlation function $C(\Delta\phi)$ for the associated DY pair and pion production in pA collisions at the LHC ($\sqrt{s} = 5.02$ TeV) for different mass numbers A.

larger Q_s, one observes that the single-particle inclusive cross section in the denominator of Eq. (17) is enhanced, while the two-particle correlated cross section [in the numerator of Eq. (17)] is suppressed. As a consequence, $C(\Delta\phi)$ decreases with an increase of the saturation scale.

Our predictions for the RHIC and LHC energies and pPb collisions are presented in Fig. 11, considering small and large dilepton invariant masses. Our results for small invariant masses, shown in the upper and middle panels, agree with those presented in Refs. [12,13]. On the other hand, our predictions for the correlation function for large invariant masses (lower panel) are at variance with the results obtained in Ref. [12] for pp collisions. We also predict a double-peak structure for large invariant masses in pPb collisions. As discussed before, in pA collisions the saturation scale is amplified by a factor of $A^{1/3}$, implying larger values for the average transverse momentum acquired by the quark in its multiple scatterings off the target. Moreover, the typical transverse momentum of the produced particles in pA collisions at $\sqrt{s} = 5.02$ TeV is smaller that in pp collisions at $\sqrt{s} = 14$ TeV. As a consequence, the impact of gluonic interactions in the produced quark is larger in pPb than in pp collisions. It implies a certain imbalance of the back-to-back photon-quark jets also for large invariant masses in pA collisions, washing out the intrinsic correlations and thus generating the double-peak structure observed in Fig. 11. The away-side peak is strongly suppressed at forward rapidities and the double-peak structure is present in the kinematic range probed by the RHIC and the LHC. Consequently, we believe that our predictions can be compared with future experimental analyses. If experimentally confirmed, this decorrelation and the double-peak structure are important probes of the underlying saturation physics.

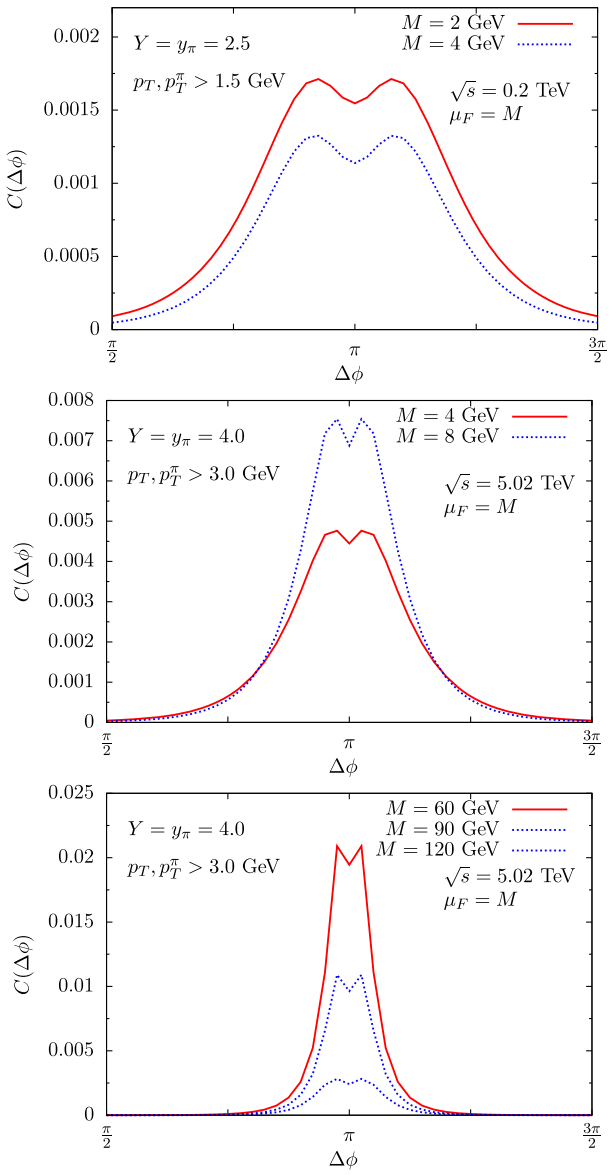

FIG. 11. The correlation function $C(\Delta\phi)$ for the associated DY pair and pion production in pPb collisions at RHIC ($\sqrt{s} = 0.2$ TeV) and LHC ($\sqrt{s} = 5.02$ TeV) energies and different values of the dilepton invariant mass.

A more elaborate study of the double-peak structure in the correlation function requires a multidimentional numerical analysis of the $C(\Delta\phi)$ function at different pion and dilepton rapidities, transverse momenta, and dilepton invariant mass as well as experimental cuts. Besides, it would be instructive to investigate how the ISI, GS, and coherence effects influence this function in various models for unintegrated gluon distributions. These questions are the subject of a separate big project which can be planned for the future, provided that the corresponding experimental data become available.

IV. SUMMARY

In this paper, we carried out an extensive phenomenological analysis of the inclusive DY $\gamma^*/Z^0 \to l\bar{l}$ process in pA collisions within the color dipole approach. Specifically, the inclusion of the Z^0 contribution enabled us to study for the first time the impact of the nuclear effects at large invariant dilepton masses. Distinct from hadron production, the DY reaction in pA collisions is a very effective tool for studying of nuclear effects since no final state interactions are expected involving either energy loss or absorption. For this reason, the DY process represents a direct and clean probe of the initial-state medium effects, not only in pA interactions but also in heavy ion collisions.

The analysis of the DY process off nuclei in different kinematic regions allowed us to investigate the magnitude of particular nuclear effects. In this paper, the contribution of the saturation, GS, and ISI effects in DY observables were estimated by considering the kinematical range probed at the RHIC and the LHC. The corresponding predictions for the dilepton invariant mass and transverse momentum differential distributions were compared with

available data at the LHC and a reasonable agreement was found. Moreover, the invariant mass, rapidity, and transverse momentum dependencies of the nucleus-to-nucleon ratio of production cross sections, $R_{pA} = \sigma_{pA}^{\mathrm{DY}}/(A \cdot \sigma_{pp}^{\mathrm{DY}})$, were estimated.

Our results demonstrated that the ratio R_{pA} is strongly modified by the GS and ISI effects. In particular, we found that both GS and ISI effects cause a significant suppression in DY production. While the GS effects dominated at a small Bjorken x in the target, the ISI effects [in accordance with Eq. (16)] became effective at large transverse momenta p_T and invariant masses $M_{l\bar{l}}$ of dilepton pairs as well as at a large Feynman variable x_F (or forward rapidities). Consequently, at forward rapidities in some kinematic regions at the LHC one can investigate only a mixing of both (GS and ISI) effects—even at large p_T values. In contrast to other inclusive processes, the advantage of the DY reaction is due to an elimination of the GS-ISI mixing by a reduction of the coherence effects at larger values of the dilepton invariant mass. Then, an investigation of nuclear suppression at large p_T represents a clear manifestation of net ISI effects—even at forward rapidities, as is demonstrated in Fig. 9. Thus, such a study of nuclear suppression at large dilepton invariant masses, transverse momenta, and rapidities—especially at the LHC energy—favors the DY process as an effective tool for the investigation of ISI effects.

In addition, we analyzed the correlation function $C(\Delta\phi)$ in the azimuthal angle $\Delta\phi$ between the produced dilepton and a forward pion which results from a fragmentation from a projectile quark radiating from the virtual gauge boson. The corresponding observable has been studied at various energies in pA collisions in both the low and high dilepton invariant mass ranges as well as at different rapidities of final states. We found a characteristic double-peak structure of the correlation function around $\Delta\phi \simeq \pi$ at various dilepton mass values and for a very forward pion. Our results indicated that a measurement of the correlation function at different energies at the RHIC and the LHC can be useful for probing the underlying dynamics by setting even stronger constraints on the saturation physics. Finally, our results demonstrated that the study of the DY reaction in pA collisions is ideal for probing the nuclear effects expected to be present at high energies and for large nuclei.

ACKNOWLEDGMENTS

E. B. is supported by CAPES and CNPq (Brazil), Contracts No. 2362/13-9 and No. 150674/2015-5. V. P. G. has been supported by CNPq, CAPES, and FAPERGS, Brazil. R. P. is supported by the Swedish Research Council, Contract No. 621-2013-428. J. N. and M. K. are partially supported by Grant No. 13-20841S of the Czech Science Foundation (GAČR) and by Grant No. MŠMT LG15001. J. N. is supported by the Slovak Research and Development Agency APVV-0050-11 and by the Slovak Funding Agency, Grant No. 2/0020/14.

[1] C. A. Salgado *et al.*, Proton-nucleus collisions at the LHC: Scientific opportunities and requirements, J. Phys. G **39**, 015010 (2012).

[2] J. C. Peng and J. W. Qiu, Novel phenomenology of parton distributions from the Drell-Yan process, Prog. Part. Nucl. Phys. **76**, 43 (2014).

[3] B. Z. Kopeliovich, in *Proceedings of the International Workshop XXIII on Gross Properties of Nuclei and Nuclear Excitations, Hirschegg, Austria, 1995*, edited by H. Feldmeyer and W. Nörenberg (Gesellschaft Schwerionenforschung, Darmstadt, Germany, 1995), p. 385.

[4] S. J. Brodsky, A. Hebecker, and E. Quack, The Drell-Yan process and factorization in impact parameter space, Phys. Rev. D **55**, 2584 (1997).

[5] B. Z. Kopeliovich, A. Schafer, and A. V. Tarasov, Bremsstrahlung of a quark propagating through a nucleus, Phys. Rev. C **59**, 1609 (1999).

[6] B. Z. Kopeliovich, J. Raufeisen, and A. V. Tarasov, The color dipole picture of the Drell-Yan process, Phys. Lett. B **503**, 91 (2001).

[7] B. Z. Kopeliovich, J. Raufeisen, A. V. Tarasov, and M. B. Johnson, Nuclear effects in the Drell-Yan process at very high-energies, Phys. Rev. C **67**, 014903 (2003).

[8] J. Raufeisen, J. C. Peng, and G. C. Nayak, Parton model versus color dipole formulation of the Drell-Yan process, Phys. Rev. D **66**, 034024 (2002); M. B. Johnson, B. Z. Kopeliovich, M. J. Leitch, P. L. McGaughey, J. M. Moss, I. K. Potashnikova, and I. Schmidt, Nuclear broadening of transverse momentum in Drell-Yan reactions, Phys. Rev. C **75**, 035206 (2007); M. B. Johnson, B. Z. Kopeliovich, and I. Schmidt, Cronin effect in the Drell-Yan reaction, Phys. Rev. C **75**, 064905 (2007).

[9] M. A. Betemps, M. B. G. Ducati, and M. V. T. Machado, Unitarity corrections to the Drell-Yan process in the target rest frame, Phys. Rev. D **66**, 014018 (2002); M. A. Betemps, M. B. G. Ducati, M. V. T. Machado, and J. Raufeisen, Investigating the Drell-Yan transverse momentum distribution in the color dipole approach, Phys. Rev. D **67**, 114008 (2003); M. A. Betemps and M. B. G. Ducati, Dilepton low p_T suppression as an evidence of the color glass condensate, Phys. Rev. D **70**, 116005 (2004); Using dileptons to probe the color glass condensate, Phys. Lett. B **636**, 46 (2006); M. A. Betemps, M. B. G. Ducati, and E. G. de Oliveira,

Dilepton distributions at backward rapidities, Phys. Rev. D **74**, 094010 (2006); M. B. G. Ducati and E. G. de Oliveira, Backward dilepton production in color dipole and parton models, Phys. Rev. D **81**, 054015 (2010); M. B. G. Ducati, M. T. Griep, and M. V. T. Machado, Study on the low mass Drell-Yan production at the CERN LHC within the dipole formalism, Phys. Rev. D **89**, 034022 (2014).

[10] R. S. Pasechnik, B. Z. Kopeliovich, and I. K. Potashnikova, Diffractive gauge bosons production beyond QCD factorisation, Phys. Rev. D **86**, 114039 (2012).

[11] E. A. F. Basso, V. P. Goncalves, and M. Rangel, Inclusive gauge boson production in the color dipole formalism, Phys. Rev. D **90**, 094025 (2014).

[12] E. Basso, V. P. Goncalves, J. Nemchik, R. Pasechnik, and M. Sumbera, Drell-Yan phenomenology in the color dipole picture revisited, Phys. Rev. D **93**, 034023 (2016).

[13] A. Stasto, B-W Xiao, and D. Zaslavsky, Drell-Yan lepton-pair-jet correlation in *pA* collisions, Phys. Rev. D **86**, 014009 (2012).

[14] F. Gelis, E. Iancu, J. Jalilian-Marian, and R. Venugopalan, The color glass condensate, Annu. Rev. Nucl. Part. Sci. **60**, 463 (2010); E. Iancu and R. Venugopalan, in *Quark-Gluon Plasma*, edited by R. C. Hwa, Advanced Series on Directions in High Energy Physics Vol. 6 (World Scientific, Singapore, 1990); H. Weigert, Evolution at small x_{Bj}: The color glass condensate, Prog. Part. Nucl. Phys. **55**, 461 (2005); J. Jalilian-Marian and Y. V. Kovchegov, Saturation physics and deuteron-gold collisions at RHIC, Prog. Part. Nucl. Phys. **56**, 104 (2006); J. L. Albacete and C. Marquet, Gluon saturation and initial conditions for relativistic heavy ion collisions, Prog. Part. Nucl. Phys. **76**, 1 (2014).

[15] J. Jalilian-Marian, A. Kovner, L. McLerran, and H. Weigert, Intrinsic glue distribution at very small *x*, Phys. Rev. D **55**, 5414 (1997); J. Jalilian-Marian, A. Kovner, A. Leonidov, and H. Weigert, Wilson renormalization group for low *x* physics: Towards the high density regime, Phys. Rev. D **59**, 014014 (1998); J. Jalilian-Marian, A. Kovner, and H. Weigert, Wilson renormalization group for low *x* physics: Gluon evolution at finite parton density, Phys. Rev. D **59**, 014015 (1998); J. Jalilian-Marian, A. Kovner, A. Leonidov, and H. Weigert, Unitarization of gluon distribution in the doubly logarithmic regime at high density, Phys. Rev. D **59**, 034007 (1999); A. Kovner, J. Guilherme Milhano, and H. Weigert, Relating different approaches to nonlinear QCD evolution at finite gluon density, Phys. Rev. D **62**, 114005 (2000); H. Weigert, Unitarity as small Bjorken *x*, Nucl. Phys. **A703**, 823 (2002); E. Iancu, A. Leonidov, and L. McLerran, Nonlinear gluon evolution in the color glass condensate: I, Nucl. Phys. **A692**, 583 (2001); E. Ferreiro, E. Iancu, A. Leonidov, and L. McLerran, Nonlinear gluon evolution in the color glass condensate: II, Nucl. Phys. **703**, 489 (2002).

[16] I. I. Balitsky, Factorization for High-Energy Scattering, Phys. Rev. Lett. **81**, 2024 (1998); Effective field theory for the small-x evolutionPhys. Lett. B **518**, 235 (2001); I. I. Balitsky and A. V. Belitsky, Nonlinear evolution in high-density QCD, Nucl. Phys. **B629**, 290 (2002).

[17] Y. V. Kovchegov, Small-*x* F_2 structure function of a nucleus including multiple Pomeron exchanges, Phys. Rev. D **60**, 034008 (1999); Y. V. Kovchegov, Unitarization of the BFKL Pomeron on a nucleus, Phys. Rev. D **61**, 074018 (2000).

[18] K. J. Golec-Biernat and A. M. Stasto, On solutions of the Balitsky-Kovchegov equation with impact parameter, Nucl. Phys. **B668**, 345 (2003); J. Berger and A. Stasto, Numerical solution of the nonlinear evolution equation at small *x* with impact parameter and beyond the LL approximation, Phys. Rev. D **83**, 034015 (2011); J. Berger and A. Stasto, Small-*x* nonlinear evolution with impact parameter and the structure function data, Phys. Rev. D **84**, 094022 (2011).

[19] E. R. Cazaroto, F. Carvalho, V. P. Goncalves, and F. S. Navarra, Could saturation effects be visible in a future electron-ion collider?, Phys. Lett. B **671**, 233 (2009).

[20] V. P. Goncalves, M. S. Kugeratski, M. V. T. Machado, and F. S. Navarra, Exclusive vector meson production in electron-ion collisions, Phys. Rev. C **80**, 025202 (2009).

[21] E. R. Cazaroto, F. Carvalho, V. P. Goncalves, M. S. Kugeratski, and F. S. Navarra, Exclusive processes in electron-ion collisions, Phys. Lett. B **696**, 473 (2011).

[22] F. Carvalho, V. P. Goncalves, F. S. Navarra, and E. G. de Oliveira, Nuclear shadowing in deep-inelastic scattering on nuclei: Comparing predictions of three unitarization schemes, Phys. Rev. C **87**, 065205 (2013).

[23] V. P. Goncalves and D. S. Pires, Deeply virtual Compton scattering at small-*x* in future electron-ion colliders, Phys. Rev. C **91**, 055207 (2015).

[24] V. P. Goncalves, F. S. Navarra, and D. Spiering, Diffractive ρ production at small *x* in future electron-ion colliders, arXiv:1510.01512.

[25] B. Z. Kopeliovich, L. I. Lapidus, and A. B. Zamolodchikov, Dynamics of color in hadron diffraction on nuclei, JETP Lett. **33**, 595 (1981).

[26] N. Armesto, A simple model for nuclear structure functions at small x in the dipole picture, Eur. Phys. J. C **26**, 35 (2002).

[27] H. De Vries, C. W. De Jager, and C. De Vries, Nuclear charge-density-distribution parameters from elastic electron scattering, At. Data Nucl. Data Tables **36**, 495 (1987).

[28] V. N. Gribov, Interaction of gamma quanta and electrons with nuclei at high-energies, Zh. Eksp. Teor. Fiz. **57**, 1306 (1969) [Sov. Phys. JETP **30**, 709 (1970)].

[29] K. J. Golec-Biernat and M. Wusthoff, Saturation effects in deep inelastic scattering at low Q^2 and its implications on diffraction, Phys. Rev. D **59**, 014017 (1998).

[30] E. Iancu, K. Itakura, and S. Munier, Saturation and BFKL dynamics in the HERA data at small-x, Phys. Lett. B **590**, 199 (2004).

[31] D. Kharzeev, Y. V. Kovchegov, and K. Tuchin, Nuclear modification factor in $d+\mathrm{Au}$ collisions: onset of suppression in the color glass condensate, Phys. Lett. B **599**, 23 (2004).

[32] A. Dumitru, A. Hayashigaki, and J. Jalilian-Marian, The color glass condensate and hadron production in the forward region, Nucl. Phys. **A765**, 464 (2006).

[33] V. P. Goncalves, M. S. Kugeratski, M. V. T. Machado, and F. S. Navarra, Saturation physics at HERA and RHIC: An unified description, Phys. Lett. B **643**, 273 (2006).

[34] D. Boer, A. Utermann, and E. Wessels, Geometric scaling at RHIC and LHC, Phys. Rev. D **77**, 054014 (2008).

[35] H. Kowalski, L. Motyka, and G. Watt, Exclusive diffractive processes at HERA within the dipole picture, Phys. Rev. D **74**, 074016 (2006); G. Watt and H. Kowalski, Impact parameter dependent color glass condensate dipole model, Phys. Rev. D **78**, 014016 (2008).

[36] J. T. de Santana Amaral, M. B. Gay Ducati, M. A. Betemps, and G. Soyez, γ^{*p} cross section from the dipole model in momentum space, Phys. Rev. D **76**, 094018 (2007); E. A. F. Basso, M. B. G. Ducati, and E. G. de Oliveira, Inclusive hadron and photon production at the LHC in dipole momentum space, Phys. Rev. D **87**, 074023 (2013).

[37] G.Soyez, Saturation QCD predictions with heavy quarks at HERA, Phys. Lett. B **655**, 32 (2007).

[38] J. Bartels, K. Golec-Biernat, and H. Kowalski, Modification of the saturation model: Dokshitzer-Gribov-Lipatov-Altarelli-Parisi evolution, Phys. Rev. D **66**, 014001 (2002).

[39] H. Kowalski and D. Teaney, Impact parameter dipole saturation model, Phys. Rev. D **68**, 114005 (2003).

[40] A. H. Rezaeian, M. Siddikov, M. Van de Klundert, and R. Venugopalan, Analysis of combined HERA data in the impact-parameter dependent saturation model, Phys. Rev. D **87**, 034002 (2013).

[41] A. Rezaeian and I. Schmidt, Impact-parameter dependent color glass condensate dipole model and new combined HERA data, Phys. Rev. D **88**, 074016 (2013).

[42] V. N. Gribov and L. N. Lipatov, Deep inelastic e p scattering in perturbation theory , Sov. J. Nucl. Phys. **15**, 438 (1972); G. Altarelli and G. Parisi, Asymptotic freedom in parton language, Nucl. Phys. **B126**, 298 (1977); Yu. L. Dokshitzer, Calculation of the Structure Functions for Deep Inelastic Scattering and $e+e-$ Annihilation by Perturbation Theory in Quantum Chromodynamics, Sov. Phys. JETP **46**, 641 (1977).

[43] F. D. Aaron *et al.* (H1 and ZEUS Collaborations), Combined measurement and QCD analysis of the inclusive $e^{+-}p$ scattering cross sections at HERA, J. High Energy Phys. 01 (2010) 109; H. Abramowicz *et al.* (H1 and ZEUS Collaborations), Combination and QCD analysis of charm production cross section measurements in deep-inelastic ep scattering at HERA, Eur. Phys. J. C **73**, 2311 (2013).

[44] J. L. Albacete, N. Armesto, J. G. Milhano, and C. A. Salgado, Nonlinear QCD meets data: A global analysis of lepton-proton scattering with running coupling Balitsky-Kovchegov evolution, Phys. Rev. D **80**, 034031 (2009).

[45] B. Z. Kopeliovich, A. Schaefer, and A. V. Tarasov, Nonperturbative effects in gluon radiation and photoproduction of quark pairs, Phys. Rev. D **62**, 054022 (2000); B. Z. Kopeliovich, J. Nemchik, and A. Schaefer, Color transparency versus quantum coherence in electroproduction of vector mesons off nuclei, Phys. Rev. C **65**, 035201 (2002); B. Z. Kopeliovich, J. Nemchik, I. K. Potashnikova, and I. Schmidt, Gluon shadowing in DIS off nuclei, J. Phys. G **35**, 115010 (2008).

[46] D. de Florian and R. Sassot, Nuclear parton distributions at next to leading order, Phys. Rev. D **69**, 074028 (2004); M. Hirai, S. Kumano, and T. H. Nagai, Nuclear parton distribution functions and their uncertainties, Phys. Rev. C **70**, 044905 (2004).

[47] B. Z. Kopeliovich, J. Nemchik, I. K. Potashnikova, M. B. Johnson, and I. Schmidt, Breakdown of QCD factorization at large Feynman x, Phys. Rev. C **72**, 054606 (2005); B. Z. Kopeliovich, J. Nemchik, I. K. Potashnikova, and I. Schmidt, Energy conservation in high-pT nuclear reactions, Int. J. Mod. Phys. E **23**, 1430006 (2014).

[48] S. S. Adler *et al.* (PHENIX Collaboration), Centrality Dependence of π^0 and η Production at Large Transverse Momentum in $\sqrt{s_{\rm NN}} = 200$ GeV $d+$Au Collisions, Phys. Rev. Lett. **98**, 172302 (2007); S. S. Adler *et al.* (PHENIX Collaboration), Measurement of Direct Photons in Au + Au Collisions at $\sqrt{s_{\rm NN}} = 200$ GeV, Phys. Rev. Lett. **109**, 152302 (2012).

[49] S. Afanasiev *et al.* (PHENIX Collaboration), Measurement of Direct Photons in Au + Au Collisions at $\sqrt{s_{\rm NN}} = 200$ GeV, Phys. Rev. Lett. **109**, 152302 (2012); T. Sakaguchi, Measurement of electro-magnetic radiation at RHIC-PHENIX, Nucl. Phys. **A805**, 355c (2008).

[50] I. Arsene *et al.* (BRAHMS Collaboration), Evolution of the Nuclear Modification Factors with Rapidity and Centrality in $d+$Au Collisions at $\sqrt{s_{\rm NN}} = 200$ GeV, Phys. Rev. Lett. **93**, 242303 (2004); J. Adams *et al.* (STAR Collaboration), Forward Neutral Pion Production in $p+p$ and $d+$Au Collisions at $\sqrt{s_{\rm NN}} = 200$ GeV, Phys. Rev. Lett. **97**, 152302 (2006).

[51] H. L. Lai, M. Guzzi, J. Huston, Z. Li, P. M. Nadolsky, J. Pumplin, and C. P. Yuan, New parton distributions for collider physics, Phys. Rev. D **82**, 074024 (2010).

[52] E. Basso, C. Bourrely, R. Pasechnik, and J. Soffer, The Drell-Yan process as a testing ground for parton distributions up to LHC, Nucl. Phys. **A948**, 63 (2016).

[53] V. Khachatryan *et al.* (CMS Collaboration), Study of Z boson production in pPb collisions at $\sqrt{s_{\rm NN}} = 5.02$ TeV, arXiv:1512.06461.

[54] G. Aad *et al.* (ATLAS Collaboration), Z boson production in $p+$Pb collisions at $\sqrt{s_{NN}} = 5.02$ TeV measured with the ATLAS detector, Phys. Rev. C **92**, 044915 (2015).

[55] J. Jalilian-Marian and A. H. Rezaeian, Prompt photon production and photon-hadron correlations at RHIC and the LHC from the color glass condensate, Phys. Rev. D **86**, 034016 (2012); A. H. Rezaeian, Semi-inclusive photon-hadron production in pp and pA collisions at RHIC and LHC, Phys. Rev. D **86**, 094016 (2012).

[56] B. A. Kniehl, G. Kramer, and B. Potter, Fragmentation functions for pions, kaons, and protons at next-to-leading order, Nucl. Phys. **B582**, 514 (2000).